NeuroImage 45 (2009) 769–777

Contents lists available at ScienceDirect

NeuroImage

journal homepage: www.elsevier.com/locate/ynimg

The effect of template choice on morphometric analysis of pediatric brain data ☆

Uicheul Yoon [a], Vladimir S. Fonov [a], Daniel Perusse [b], Alan C. Evans [a,*]
Brain Development Cooperative Group [1]

[a] McConnell Brain Imaging Centre, Montreal Neurological Institute, McGill University, Montreal, Quebec, H3A 2B4, Canada
[b] The Research Centre at the Sainte Justine Hospital, Montreal, Canada

ARTICLE INFO

Article history:
Received 20 May 2008
Reevised 12 December 2008
Accepted 17 December 2008
Available online 6 January 2009

Keywords:
Magnetic resonance imaging
Pediatric brain template
Spatial normalization
Tissue classification
Cortical surface
Parcellation

ABSTRACT

The present study investigated the "template effect" on the morphometric analysis of a pediatric brain MRI database obtained from 8-year-old children through various measures of surface and volumetric morphologies. We first constructed an age-appropriate template from an independent set of pediatric brain images and then compared it with a well-known adult brain template, the ICBM152, in terms of the morphometric features that resulted from our pediatric database. The individual cortical surface acquired based on the pediatric template exhibited, on average, a significantly thinner cortex (−1.66±1.60%, $t=-15.18$), larger cortical surface areas (0.31±0.70%, $t=6.52$), and a higher degree of cortical folding (0.08±0.13%, $t=8.72$) while compared with those based on the adult template. We also found a significant increase in the cerebrospinal fluid volume (−2.63±4.84) for the adult template based brains and the cortical gray matter (GM) volume (6.10±7.81) for the pediatric template based brains. The cross-correlation of pediatric template based individual brain data (0.95 without brain mask) was significantly higher than those of adult template based (0.88) and the amount of deformation during non-linear spatial normalization was significantly reduced when using the pediatric template (average magnitude of deformation in the cortical GM class: 1.71 mm vs. 2.23 mm, $t=12.39$). In addition, an "internal" pediatric template, taken from the study subjects themselves, was generated and compared with the "external" pediatric template for reference. There was no significant difference between these two pediatric brain templates and associated tissue probability maps. The results show that it is necessary to be cautious when interpreting results from pediatric imaging studies based on adult reference data.

Introduction

Since the individual variability in brain mapping studies has to be minimized in order to facilitate intra- and inter-individual comparisons and to generalize specific findings, a human brain template aligned in the standardized space is an indispensable tool (Mazziotta et al., 1995). Spatial normalization which minimizes the anatomical variability between studied brain data is achieved by transforming the individual brain image to a common template in stereotaxic space. The brain template contains *a priori* knowledge about the human brain, which is useful for the spatial normalization of a new brain image. The Talairach and Tournoux (1988) reference frame is widely used in such normalization procedures. It relies on aligning the anterior and posterior commissures and the interhemispheric plane of the source image with the brain template. However, it has a number of limitations. The most significant one is that the Talairach system does not clearly represent the various peculiarities of *in vivo* subjects since it was acquired from a single postmortem brain (Toga and Thompson, 2001). Another well-known brain template for spatial normalization is the ICBM152 (International Consortium for Brain Mapping), which was generated by averaging anatomical magnetic resonance imaging (MRI) data of 152 healthy normal adults (86 male, 66 female, 18–44 years old) after corrections for overall brain size and orientation (Collins et al., 1994; Grabner et al., 2006). Although the ICBM152 template is intuitively better suited for spatial normalization, it remains to be established whether it is applicable to data from subjects outside of the age range or with abnormal neuropathological conditions. In particular, the use of this template in the spatial normalization of pediatric brains is still questionable because of the large difference in size, composition and shape between the pediatric brain and the adult brain (Burgund et al., 2002; Courchesne et al., 2000; Hoeksma et al., 2005; Lange et al., 1997; Muzik et al., 2000; Wilke et al., 2008, 2002, 2003).

Several studies have found that there are some inevitable problems when pediatric brains are aligned to an adult brain template (ABT) (Burgund et al., 2002; Muzik et al., 2000). Using a standard ABT,

☆ Template for Pediatric Data.
* Corresponding author. Fax: +1 514 398 8948.
E-mail address: alan.evans@mcgill.ca (A.C. Evans).
URL: http://www.bic.mni.mcgill.ca/alan/ (A.C. Evans).
[1] See Appendix A for author list.

1053-8119/$ – see front matter © 2009 Elsevier Inc. All rights reserved.
doi:10.1016/j.neuroimage.2008.12.046

contours of spatially normalized MRI volumes derived from the pediatric group were more variable than those obtained from the adult population (Muzik et al., 2000). Even though it has been suggested to be sufficiently accurate for coarse-resolution (>5 mm) functional MRI data (Burgund et al., 2002), these errors become more evident when a higher resolution structural or functional data is applied. In a simple statistical test for the regional group intensity variance after registration, it was shown that the alignment of pediatric brains to the ABT was less successful with significant intensity variance differences in the white matter and thalamic regions (Hoeksma et al., 2005). In addition, serious misclassification of pediatric brain tissue in several regions has also been reported due to the inappropriate use of *a priori* information obtained from an adult population (Wilke et al., 2003). Therefore, it is vital to use accurate reference data, especially for the analysis of a pediatric population (Good et al., 2001).

There have been several approaches to evaluate the effect of using a pediatric brain template (PBT) versus an ABT on the spatial normalization of pediatric brain images (Machilsen et al., 2007; Wilke et al., 2002, 2003). To the best of our knowledge, however, there has not been any research to assess the effect of different brain templates on cortical surface morphology. Even though the affine scaling parameter should not be correlated with age if brain masking was employed during the spatial normalization, non-linear deformations were found to be locally correlated with age in the parietal and frontal areas and the total amount of volume change was significantly lower when using a PBT (Wilke et al., 2002). However, it is important to note that the influence of expected similarities between individual pediatric brain and PBT might be incorporated in the result since the template was based on the average of the same pediatric dataset. In addition, the Wilke et al. (2002) PBT included a large variability in normal age-related brain morphology by using data from children over a wide age range (5 to 18 years old). This heterogeneity might introduce more variations to the normalization of individual pediatric brain images for a particular age within that range. A more age-appropriate PBT may yield a mathematically better correspondence and a diminishing disagreement in probability values for tissue classification.

The purpose of this study is to investigate the template effect on the morphometric analysis for a large sample of pediatric brain data. In the following Materials and methods section, we will present the detailed procedure to construct a PBT for a specific age (8 years old) and introduce several processing steps based on each template including linear and non-linear spatial normalization, tissue classification, and extraction of cortical surface. Various measures with regard to surface and volumetric characteristics are also presented for a quantitative comparison between templates.

Materials and methods

Subjects and image acquisition

Subjects were drawn from the Quebec Newborn Twin Study (QNTS) which is an ongoing longitudinal study of twins who were recruited at birth between 1 April, 1995 and 31 December, 1998 in the Province of Quebec, Canada. Two hundred eight subjects (8.40±0.11 years old) took part in the study (86 males and 122 females). All 8-year-old children were scanned using the same 1.5 T MRI scanner (Magnetom Vision, Siemens Electric, Erlangen, Germany). The MRI sequences acquired were (i) T1-weighted, sagittal, fast low-angle shot (FLASH) of the whole head, designed to optimally discriminate between brain tissues (T_E=10 ms, T_R=22 ms, flip angle=30°, 160 contiguous slices; matrix size=224×256; 1×1×1 mm^3 voxels), and (ii) the axial PD and T2 sequence of the whole head for clinical evaluation and better cerebral masking (T_E=17/102 ms, T_R=3516 ms, flip angle=180°, 81 contiguous slices; matrix size=256×256; 1×1×2 mm^3 voxels). All of the raw data underwent a series of visual quality controls which included the level of intensity inhomogeneity within/between slices, the amount of movement artifacts and geometric distortions (Evans and Brain Development Cooperative Group, 2006). Written informed consent was obtained from parents after full explanation of the study aims and procedures. The study protocol was approved by the scientific and ethics committees of Sainte Justine and Notre Dame Hospitals in Montreal, Canada.

Construction of pediatric templates

The study by Wilke et al. (2003) created a pediatric template from the study population, i.e. "internal" pediatric template (iPBT). The present work is concerned with the difference between the effects of two "external" templates and the issue of adult–pediatric brain anatomy. Comparing an iPBT with an external ABT would introduce a confusion of "external" vs. "internal" into the analysis of "adult" vs. "pediatric". To avoid any influence of additional similarity between study subjects and template on the result, the external pediatric template (ePBT) was generated from an independent set of pediatric brain images. Since a more age-appropriate ePBT may yield a better correspondence among individual datasets, MR images of 53 healthy children (23 males, 30 females, 8.97±0.56 years old) were selected from the Pediatric MRI Data Repository created by the NIH MRI Study of Normal Brain Development (Evans and Brain Development Cooperative Group, 2006). Even though more than 400 subjects were available from this longitudinal study of typically developing children, only 53 children from 8 to 9 years old were selected in order to match the age distribution of subjects for this study. A whole-brain, 3D T1-weighted spoiled gradient recalled (SPGR) echo sequence was performed with the following parameters: T_E=10–11 ms, T_R=22–25 ms, flip angle=30°, 124 contiguous sagittal slices; matrix size=256×256; 1×1×1 mm^3 voxels (Evans and Brain Development Cooperative Group, 2006). The two-phase procedure for generating the ePBT was the same approach as was used for the ICBM152 template, i.e. a symmetric iterative group volumetric template created by including left–right flipped versions of all the original images and constraining the evolving template (Grabner et al., 2006; Miller et al., 1997). The ICBM152 template was chosen as the ABT in this study and used as a reference model for linear registration and intensity normalization, which is based on the median values, to correct the inter-subject intensity variations.

Phase 1 (linear)

The intra-slice intensity variations of each dataset in the ePBT ensemble introduced by inhomogeneity in the radio frequency field were corrected by histogram spline sharpening. The inter-slice intensity variations were clamped by thresholding the image intensity gradient curve in all three planes using N3 (Sled et al., 1998). In preparation for the following procedure, each image was initially aligned to its own mirror image about the midline using a rigid-body transformation. The resulting two transformations were then averaged and the resultant transformation applied to the original image. Once all the subject volumes were aligned, they were again flipped over the midline. Both aligned and aligned-flipped images from each subject were linearly registered to the initial model (ICBM152) using the hierarchical fitting procedure to reduce the probability of local minima (Collins et al., 1994). The resulting linear transformation for the aligned-flipped image was then flipped about the X-axis in order to be averaged with the transformation for the aligned image. Afterwards, the averaged transformation was applied to the aligned image and a flipped version of the averaged transformation to the aligned-flipped image. Then all the resulting data were averaged as well as all transformations. To ensure no bias from the initial reference model, the inverted average scaling factor was then applied to the averaged data which yielded the next generation model. This was done in order to scale the model into the average size of all data used.

Phase 2 (non-linear)

Subsequent iterations then followed using successively higher resolution (32–2 mm in step size) of non-linear registration to match individual data to the current iteration of the reference model (Grabner et al., 2006). A general diagram of the procedures for the nth iteration is shown in Fig. 1. Using the transformation parameters from the previous iteration as a starting point, both the aligned and aligned-flipped images were non-linearly registered to the reference model generated from the previous iteration. The symmetric model was generated by averaging the mean transformed images of the aligned volumes, and used for the following iteration. In order to ensure that no bias was introduced towards a particular intermediate model during the construction of the final model, it is important to note that registration of each step began with every image in its initial space.

In order to use *a priori* information for tissue classification of pediatric MRI data, the spatial transformations derived for the raw MRI images were applied to the tissue classification maps of each individual subject such that a probability map for each tissue class was generated in the pediatric template space.

We also generated an iPBT from the 208 study subjects for reference. Since it is impossible to differentiate a true template effect from the result caused by an additional similarity when a subject is processed based on its own average, the iPBT was compared with the ePBT only in terms of the template itself and tissue probability maps. The issue of an internal vs. external PBT will be addressed further in a subsequent study.

Processing

The following pipeline image processing steps, based on both the ePBT and ABT were applied for further analysis, as described in detail elsewhere (Collins et al., 1994; Evans and Brain Development Cooperative Group, 2006; Kim et al., 2005; MacDonald et al., 2000; Sled et al., 1998; Zijdenbos et al., 2002). At first, the native MR images of all subjects were registered into each template using a linear transformation and corrected for intensity non-uniformity artifacts (Sled et al., 1998). All non-brain parts of the image including the skull and meninges were removed by an automated brain extraction algorithm (Smith, 2002). A hierarchical multi-scale non-linear fitting algorithms (ANIMAL, Collins et al., 1994) was then applied (i) to normalize the individual MR images in stereotaxic space, (ii) to provide *a priori* information i.e. tissue probability maps for subsequent tissue classification using the neural network classifier (Zijdenbos et al., 2002) and (iii) to obtain the 3D deformation vector field that maps the individual brain volume onto the template. An artificial neural network classifier was applied to identify gray matter (GM), white matter (WM) and cerebrospinal fluid (CSF). Partial volume errors due to tissue-mixing at their interfaces were estimated and corrected using trimmed minimum covariance determinant method (Tohka et al., 2004; Zijdenbos et al., 2002). Hemispheric cortical surfaces were automatically extracted from each MR volume using the Constrained Laplacian-based Automated Segmentation with Proximities (CLASP) algorithm, which reconstructs the inner cortical surface by deforming a spherical mesh onto the WM/GM boundary and then expanding the deformable model to the GM/CSF boundary (Kim et al., 2005; MacDonald et al., 2000). The accuracy of this technique had been demonstrated in a phantom-based quantitative cross-validation study, showing the best geometric and topologic accuracies and mesh characteristics of the extracted cortical surface (Lee et al., 2006). Then, we employed an iterative surface registration algorithm with an unbiased iterative group template showing enhanced anatomic detail in order to assure the correspondence at each vertex of the cortical surface model between individuals (Lyttelton et al., 2007). For regional analysis, automatic lobar parcellation which had been validated and performed efficiently in previous studies, was applied for dividing individual cortical surface into frontal, temporal, parietal and occipital lobes (Im et al., 2008; Yoon et al., 2007). Four surface morphometric

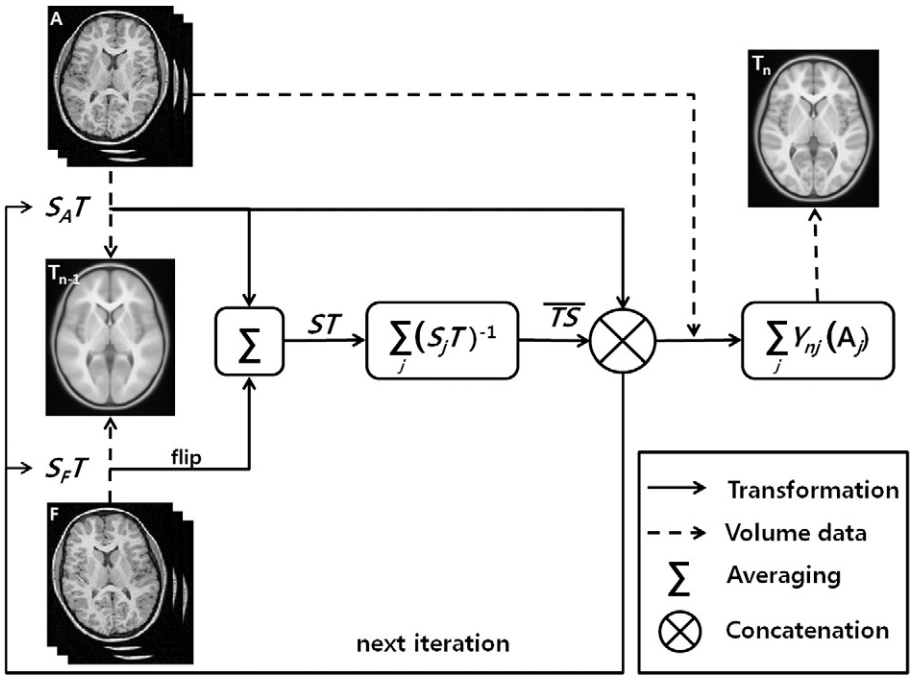

Fig. 1. A general overview of non-linear fitting and averaging procedure at *n*th iteration. Both the aligned (A) and aligned-flipped (F) images are non-linearly matched to the reference model (T_{n-1}) generated from the previous iteration using the transformation parameters (Y_{n-1}) from previous iteration as a starting point. Note that there is an important constraint on the registration, which the transformation S_FT should be equal to a flipped version of the transformation S_AT. For each subject, the resulting transformations are combined by flipping S_FT. This transformation (ST) of each subject is inverted and averaged within population. The averaged transformation ($\overline{TS}$) is then concatenated with the former transformation (S_AT) of each subject and applied to the aligned volume. Finally, the symmetric model (T_n) is generated by averaging the mean transformed images of aligned volumes, and is going to be used for the following iteration.

indices (cortical thickness, cortical area, mean gyrification index and cortical complexity) and four volumetric indices (intensity variance, cross-correlation, tissue volume size and amount of local non-linear deformation) were introduced in order to evaluate the performance of the ePBT in comparison with the ABT. Finally, we verified if there was any gender difference in template effects by subdividing the pool of subjects into male and female subgroups.

Measurement of cortical surface characteristics

Since the cortical surface models were extracted from MR volumes in stereotaxic space, the inverse transformation was applied to the individual dataset so that various morphometrics, i.e. cortical thickness, cortical area, mean gyrification index (GI) and cortical complexity can be measured in native space. The measurement in native space provided an unadjusted estimate of absolute cortical characteristics (Shaw et al., 2006). The cortical thickness was measured as the Euclidean distance between linked vertices on the inner and outer surfaces, and then averaged for each hemisphere and lobar regions for further regional analysis (Kabani et al., 2001; Lerch and Evans, 2005; MacDonald et al., 2000). An intermediate cortical surface, half-way between the inner and outer CLASP surfaces, was used for measuring the surface morphometrics as it represents a relatively unbiased representation of both sulcal and gyral regions (Van Essen et al., 2006). The cortical area was calculated in the whole hemisphere and each lobar region by summing the Voronoi area based on geodesic distances over the folded topology of the surface (Lotjonen et al., 1998). The middle cortical surface was divided into the sulcal and gyral regions by thresholding the depth map, i.e. 3D Euclidean distance from each vertex to the nearest voxel on the convex hull volume (Im et al., 2008). The threshold of the depth map was determined from the fact that the human cerebral cortex is a highly folded sheet with 60–70% of its surface area buried within folds (Van Essen and Drury, 1997; Zilles et al., 1988). The mean GI was defined as the ratio between the total surface area and the superficially exposed surface areas such as the gyral regions in each hemisphere and lobe (Zilles et al., 1988). For cortical complexity, we modified a similar idea from Thompson et al. (2005) that calculated complexity from a spherical surface mesh deformed hierarchically onto the cortex. The surface inflation technique was applied to the middle cortical surface, and then the rate of decreasing cortical areas with increasing inflation frequency (N=2–256) was estimated as the complexity by least-squares fitting of a linear model as shown below.

$$CC = 2 - d(lnCA(N))/d(lnN),$$

where $CA(N)$ represents the cortical area for the Nth inflation. Intuitively, a complexity value of larger than 2 indicates an increase in the cortical surface detail and cortical folding degree. To be consistent with other measures, the cortical complexity was measured for each hemisphere and lobar region.

Measurement of volumetric characteristics

We would also like to examine whether the choice of template influenced cortical GM volume and cortical surface morphometric indices in a similar manner, i.e. would they change in the same direction. For this purpose, the overall GM map obtained by tissue classification was sub-divided into cortical and sub-cortical regions via a sub-cortical GM stereotaxic mask.

The algorithm for spatial normalization used in this study (Collins et al., 1994) maximizes the cross-correlation between individual and template brain. A relatively low cross-correlation value with low group intensity variance after alignment denotes a structural bias in normalization, whereas a low cross-correlation value with larger variance indicates some random differences (Hoeksma et al., 2005). Furthermore, it is well-known that removal of peripheral voxels by a whole brain masking has a significant impact upon the spatial normalization process (Smith, 2002). In order to assess the adequacy of each template for spatial normalization, the voxel-wise intensity variance and the cross-correlation values after linear alignment to each template were computed with and without a brain mask.

The amount of local non-linear deformation was investigated to demonstrate which template was most appropriate for normalization of pediatric data. Smaller local changes indicate a greater similarity in shape between the individual brain and template brain. The magnitude values of the non-linear deformation vector field were determined to evaluate the effect of non-linear warping of each individual brain to the template. These deformation magnitude maps were first smoothed with a 3D Gaussian kernel (FWHM of 8 mm) to create a local weighted average of the surrounding voxels. This step also renders the data more normally distributed and increases the validity of the statistical tests (Ashburner and Friston, 2000). Next, we calculated the average and maximum magnitude values of deformation within each of tissue classes (cortical GM, sub-cortical GM, WM, CSF) to investigate the overall shape change (deformation) and to avoid the inherent multiple comparison problem in voxel-wise hypothesis testing. Finally, the class-wise values for each subject were averaged to obtain a population index for the mean magnitude of non-linear deformation.

Statistical analysis

The vertex-based maps of cortical thickness in native space were convolved with a diffusion smoothing kernel to increase the signal to noise ratio (Chung et al., 2003). A Gaussian kernel size of 30 mm FWHM was selected to maximize statistical power while minimizing false positives (Lerch and Evans, 2005). A false discovery rate (FDR) threshold of $P<0.01$ was employed to control for multiple comparisons (Genovese et al., 2002). Lobar differences of cortical surface characteristics and differences of classified tissue volume size between templates were examined with a paired t-test, while the amount of local non-linear deformation within each segmented tissue region was estimated by an independent two sample t-test.

Results

Pediatric template vs. adult template

Fig. 2 shows the non-linear symmetric brain templates and tissue probability maps of both the child and adult. It is noteworthy that our methodology for generating a symmetric template is able to adequately represent both common structures and variable subregions within the population. The ePBT is slightly larger (5.7%) in cerebral volume than the ABT, a somewhat counter-intuitive result. This is a consequence of the different proportions of GM, WM and CSF in the two populations, and the linear normalization procedure (phase 1) does not accommodate these differences because it might not introduce distortions into the resulted images. On the other hand, the ABT does show a larger ventricle and outer CSF regions than those of the ePBT (Fig. 2a). Significant developmental changes were observed in the tissue probability maps such as the reduced regional GM patterns (relative volume, ePBT: 59.1% vs. ABT: 53.1%), and increased total WM (28.2% vs. 31.1%) and CSF (12.7% vs. 15.8%) in ABT (Fig. 2b). Since the tissue probability maps were used in tissue classification as *a priori* information and the cortical surfaces were extracted from resulted tissue-classified images, several differences in the whole brain template and tissue probability maps could affect the outcomes of the morphometric analysis for pediatric brain, as detailed in the following sections.

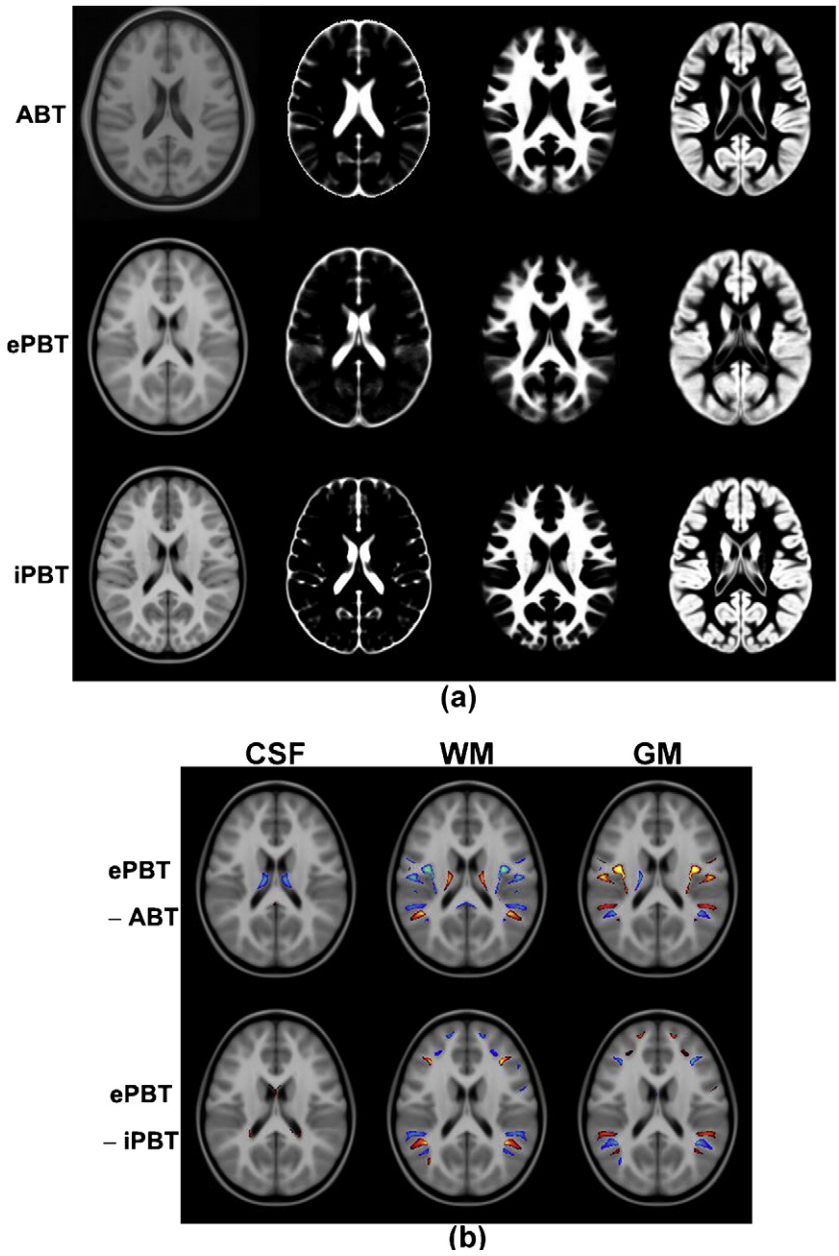

Fig. 2. (a) Brain template and associated tissue probability maps for CSF, white matter and gray matter (top: external adult template (ABT); middle: external pediatric template (ePBT); bottom: internal pediatric template (iPBT)). (b) The difference (>0.5, minimum cluster size=200 voxels) in tissue probability distribution was color-coded and superimposed upon the ePBT (top: ePBT–ABT; bottom: ePBT–iPBT). Blue represents a negative difference and red indicates a positive one. The software tool *MRIcro* was used to display the image and to set the minimum cluster size (http://www.mricro.com).

The results of the comparison between the iPBT and ePBT are also shown in Fig. 2. Contrary to the external adult–pediatric template comparison, there was no significant difference between the iPBT and ePBT, except for a slightly clearer boundary in the iPBT that could arise from a larger sample size (53 vs. 208 subjects, Fig. 2a). Even though there was a minor difference between the tissue probability maps, this could have resulted from a slight misalignment between templates rather than from a real difference (Fig. 2b). It was noticeable that the gyral patterns of each template are different even after alignment using the affine transformation. The parallel blue and red colors shown in Fig. 2b suggest a simple misalignment due to affine transformation between templates (N.B. not between subjects, which is the non-linear transformation). In addition, there were no significant differences in the relative tissue volumes (Internal vs. External: CSF: 11.3% vs. 12.7%; GM: 60.1% vs. 59.1%; WM: 28.6% vs. 28.2%).

Statistical results for cortical surface characteristics

Localized differences of cortical thickness between the ePBT and ABT are displayed in Fig. 3. The cortical thickness based on the ABT was greater in all vertices (mean difference in left hemisphere: 1.7±0.6%, right hemisphere: 1.6±0.7%). In particular, the frontal, occipital and medial regions in both hemispheres showed significant differences.

The statistical results of lobar differences in cortical surface characteristics between templates are also presented in Table 1. As expected, the mean cortical thickness based on the ABT was significantly greater in both hemispheres and all lobes. Although the female subgroup showed a slightly greater difference between templates in all brain regions except the left temporal lobe, there was no significant difference between the two subgroups. On the other hand, the cortical areas based on the ePBT were significantly larger in bilateral frontal lobes than those based on the ABT. In

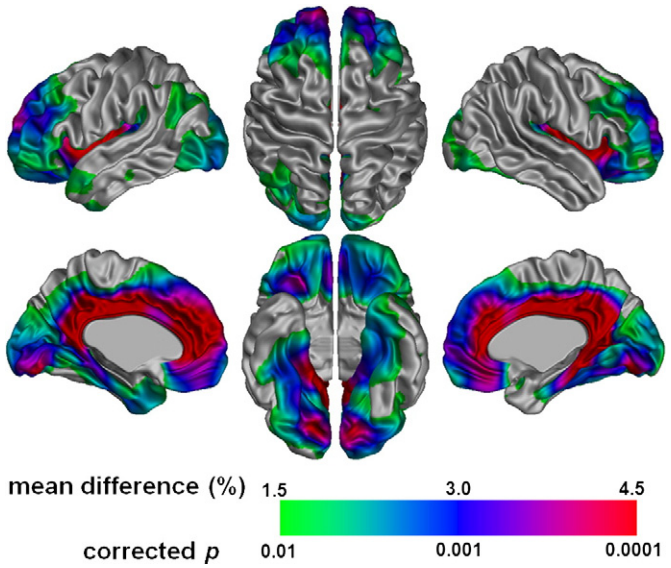

Fig. 3. Statistical map of vertex based *t*-test for the difference of cortical thickness between templates. Mean difference and corrected *p* value are color-coded and mapped onto the iterative group template which is a target model of surface registration. All of the vertices show greater thickness in the adult template.

contrast with females, the male subgroup did not exhibit any significant differences in areas for the left lobar regions. In addition, there was a significant gender difference in the left frontal lobar area ($P=0.007$). The mean GI based on the ABT was significantly greater in the left temporal lobe, and vice versa in the bilateral parietal lobes. The female subgroup showed significant differences in GI between templates for the left parietal and bilateral temporal lobes. However, the male subgroup only showed a significant difference in GI for the right parietal lobe. There was also a significant gender difference in GI for the right temporal lobe ($P=0.074$). The cortical complexities of all regions except the right occipital lobe were significantly increased in the cortical surface based on the ePBT, while there was no significant gender difference.

Statistical results for volumetric characteristics

The differences of brain tissue volumes in native space between templates are reported in Table 2. The volume of the CSF tissue class was significantly greater for the ABT while the cortical GM based on the ePBT was significantly increased. The increment of sub-cortical GM volume based on the ABT was correlated with an increase in WM volume based on the ePBT. No significant gender difference between templates was observed for the volumetric characteristics and hence those results are not reported.

Regardless of the brain mask, the cross-correlation between the individual and template brains was significantly lower for the ABT (Fig. 4), while there was no significant difference between the two templates in voxel-wise intensity variance. However, the intensity variance within the brain mask was rather low and the absolute value of the cross-correlation was increased when using a brain mask. Therefore, a brain masking procedure should be employed when pediatric imaging data is spatially normalized for further morphometric analysis. Table 2 lists the average and maximum magnitudes of the deformation field within segmented tissue regions. The average and maximum magnitude for the whole brain were 2.2 mm and 7.8 mm for the ABT and 1.7 mm and 6.5 mm for the ePBT ($P<0.001$), respectively. The necessary amount of deformation for warping pediatric data to the ABT was significantly greater in all segmented tissue regions than using the ePBT (CSF: 20.1±8.6%; GM: 23.4±7.8%; WM: 24.1±10.4%; cortical GM: 23.1±8.0%; sub-cortical GM: 21.9±17.5%).

Discussion

We have presented a detailed procedure to construct a brain template from high resolution MR images of pediatric population. The

Table 1
Cortical surface characteristics based on different templates

			Hemisphere	Frontal	Temporal	Parietal	Occipital
CT[a]	L	W	1.73±1.80	1.85±2.07	1.64±1.75	1.55±1.80	1.81±1.92
		M	1.65±1.69	1.71±1.90	1.66±1.66	1.48±1.72	1.76±1.96
		F	1.78±1.88	1.95±2.18	1.64±1.84	1.60±1.86	1.85±1.90
	R	W	1.59±1.72	1.78±1.87	1.45±1.76	1.38±1.74	1.63±1.91
		M	1.38±1.83	1.54±1.89	1.22±1.91	1.22±1.92	1.49±2.02
		F	1.74±1.64	1.95±1.85	1.62±1.63	1.50±1.60	1.73±1.83
CA	L	W	−0.31±0.96**	−0.4±1.38**	−0.15±1.74	−0.42±2.83	−0.06±2.23
		M	−0.17±0.96	−0.07±1.34[b]	0.03±1.64	−0.38±2.85	−0.23±2.09
		F	−0.41±0.94**	−0.63±1.36**	−0.28±1.80	−0.45±2.83	0.06±2.33
	R	W	−0.31±0.79**	−0.51±1.41**	0.04±1.81	−0.49±3.10	0.06±2.05
		M	−0.34±0.77**	−0.51±1.50**	−0.20±1.83	−0.44±3.15	0.17±2.18
		F	−0.30±0.81**	−0.51±1.35**	0.21±1.79	−0.52±3.07	−0.02±1.95
mGI	L	W	−0.16±3.46	−0.15±3.18	1.51±5.99**	−1.41±4.97**	−0.26±3.52
		M	−0.15±3.81	−0.12±3.48	1.39±6.30	−1.31±5.56	−0.33±3.91
		F	−0.17±3.20	−0.18±2.96	1.59±5.80*	−1.48±4.53**	−0.22±3.24
	R	W	−0.37±3.85	−0.33±3.57	1.00±5.89	−1.37±5.39**	−0.55±3.80
		M	−0.97±4.26	−0.63±3.78	−0.20±6.68[b]	−2.12±5.93**	−0.75±3.69
		F	0.05±3.49	−0.12±3.42	1.85±5.13**	−0.84±4.93	−0.41±3.89
CC	L	W	−0.08±0.18**	−0.07±0.18**	−0.05±0.16**	−0.10±0.27**	−0.06±0.32*
		M	−0.07±0.20*	−0.09±0.19**	−0.04±0.17	−0.09±0.24**	−0.02±0.34
		F	−0.09±0.18**	−0.06±0.18**	−0.06±0.14**	−0.12±0.29**	−0.08±0.30**
	R	W	−0.07±0.15**	−0.09±0.16**	−0.03±0.14**	−0.11±0.20**	−0.03±0.25
		M	−0.06±0.16**	−0.08±0.17**	−0.04±0.15	−0.11±0.19**	−0.01±0.29
		F	−0.08±0.13**	−0.10±0.15**	−0.03±0.13*	−0.12±0.21**	−0.05±0.21

All values represent a percentage of the difference between templates. Positive value indicates that a measure based on the ABT is greater than that based on the ePBT.
Note: CT: cortical thickness; CA: cortical area; mGI: mean gyrification index; CC: cortical complexity; L: left; R: right; W: whole population; M: male subgroup; F: female subgroup.
* $P<0.01$.
** $P<0.001$.
[a] Mean values of cortical thickness based on the ABT are significantly greater than those based on the ePBT regardless of lobe or population.
[b] There is significant gender difference in template effect.

Table 2
Volumetric characteristics based on different brain template in segmented tissue regions

		CSF	WM	GM	SUB_GM	COR_GM
VOL_DIFF (mm^3)		−2.63±4.84**	1.31±6.86*	5.77±8.29**	−0.33±1.02**	6.10±7.81**
AVG_MAG[a] (mm)	ABT	2.28±0.46	2.04±0.47	2.20±0.45	1.80±0.46	2.23±0.46
	ePBT	1.83±0.42	1.55±0.42	1.69±0.39	1.39±0.44	1.71±0.40
MAX_MAG[a] (mm)	ABT	6.64±1.18	6.62±1.20	6.74±1.18	6.19±1.20	6.73±1.18
	ePBT	5.58±1.24	5.47±1.29	5.64±1.23	5.19±1.19	5.60±1.23

The difference of tissue volume was calculated by subtracting a measure based on the ePBT from one based on the ABT.
Note: VOL_DIFF: volume difference; AVG: average; MAG: magnitude of deformation field; MAX: maximum; ABT: adult template; ePBT: external pediatric template; CSF: cerebrospinal fluid; WM: white matter; GM: gray matter; SUB: sub-cortical; COR: cortical.
* $P<0.01$.
** $P<0.001$.
[a] The amount for warping to the ABT is significantly greater in all regions (independent two sample t-test $P<0.001$).

constructed ePBT is larger than the ABT which is in accordance with the previous pediatric template study (Thompson et al., 2000b). The sectional view of the ePBT exhibits excellent delineation of even small morphological structures (Fig. 2). However, there are apparent differences in the tissue probability maps as the ePBT has relatively more GM, and less WM and CSF than the ABT. This is also in agreement with previous studies for normal brain development (Giedd et al., 1999; Pfefferbaum et al., 1994; Thompson et al., 2000a). While cortical and sub-cortical GM volumes show evidence of reduction after late childhood, WM volume appears to be increasing robustly into adulthood and the absolute volume of ventricular and extracerebral CSF increases substantially and almost linearly throughout the life span (Courchesne et al., 2000). One study suggested that significant tissue misclassification would be likely to occur when analyzing a pediatric sample with adult *a priori* information since a strong bias might already be inserted into the data by processing them on the basis of possibly inappropriate *a priori* information (Wilke et al., 2003). However, it was important to confirm these effects on the morphometric results by applying a PBT and its *a priori* information to an independent set of pediatric brain images as what we have accomplished in this study.

The individual cortical surface based on the ePBT was characterized by thinner cortical thickness, larger cortical surface area and higher degree of cortical folding than those based on the ABT. Since the cortical surface extraction process depends upon the results of tissue classification as mentioned above, the difference in volumes of native cortical GM observed when using the two templates (Table 2) could account for the significant difference observed in cortical thickness. Though there is no evidence of correlation between the degree of cortical surface folding and brain volume (Zilles et al., 1988), it is reasonable to presume that if two brains of different sizes (i.e. volume) have the same cortical surface area, then the smaller brain must have a higher surface folding complexity. The measurements of cortical folding pattern, mean GI and cortical complexity demonstrate a higher degree of folding for the ePBT-based pediatric brain.

While intensity variance of the pediatric data after linear alignment was negligible for both templates, the cross-correlation value for the ePBT was significantly higher than for the ABT and the amount of deformation to the ePBT was significantly less. This suggests that the ePBT is more appropriate for stereotaxic alignment of the pediatric data than the ABT. When attempting to capture the variance within a population, it is important to measure individual variance with respect to an appropriate population mean such that the total variance is minimized (Bookstein, 1997). Using the mean variances of one population (e.g. adults) to investigate another population (e.g. children) inevitably introduces a systematic bias. The more similar the individual and template is, the less deformation is needed for each individual to truly reflect the anatomical variability within the target population (Guimond et al., 2000). Table 2 shows that remarkably less average deformations are required and more accuracy is obtained when aligning the pediatric dataset to our ePBT. These results re-affirm that a specific PBT represents more accurate anatomical features of a specific pediatric population than one based on adults (Thompson et al., 2000b).

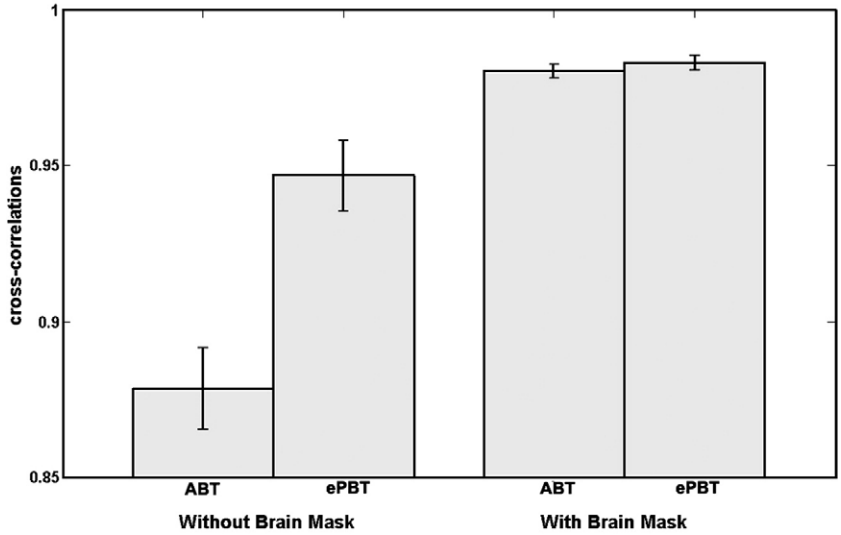

Fig. 4. Mean (standard deviation) of cross-correlation values between individual and each template with and without brain mask. Although the absolute value is increased when using brain mask, the cross-correlation with the adult template is significantly lower in both cases.

Methodological considerations

As is done when constructing MRI templates for adult brain studies, a large population is needed to create a good quality, representative template. Data used for the ePBT in this study were obtained from the Pediatric MRI Data Repository created by the NIH MRI Study of Normal Brain Development (http://www.bic.mni.mcgill.ca/nihpd/info). This is a multi-site, longitudinal study of typically developing children, ranging from newborn to young adulthood (Evans and Brain Development Cooperative Group, 2006). For that database, MRI and an extensive behavioral data were collected in a demographically-representative pediatric population. We only used 53 subjects out of 400 subjects (4.6–18.3 years old) that are matched to the age distribution of our QNTS subjects to create the ePBT described in this study. Although subjects were imaged at multiple sites, data were collected with an identical imaging protocol. This minimized the differences among images with respect to several criteria such as geometric accuracy, high contrast spatial resolution, image intensity non-uniformity, signal ghosting, and slice thickness (Evans and Brain Development Cooperative Group, 2006). This database provides the means for characterizing healthy brain maturation in relationship to behavior and serve as a source of control data for studies of childhood disorders.

We employed surface-based lobe measures for cortical folding pattern by mean of GI and complexity. Since these 3D measures were independent of the imaging plane, we avoided a shortcoming of previous GI measures related to the length of an inner and outer cortical contour in 2D slices of the brain (Zilles et al., 1988). Even though both complexity and GI are dependent upon a comparison between the whole area of cerebral cortex and the size of folded area, it is difficult to deduce a mathematical relation between those measures. The GI metric makes use of location-specific information without referring to variable spatial scales, whereas the calculation of complexity considers the surface to be smoothed at a series of different spatial scales (Kiselev et al., 2003). Two measures provide complementary information that may be useful for characterizing cortical folding and a means to detect subtle and distributed variations in anatomic structure, not apparent by visual inspection.

Although the volumetric characteristics showed no significant gender difference between the two templates, several surface characteristics, especially the cortical area in left frontal lobe and mean GI in right temporal lobe, exhibited significant gender differences (Table 2). It has been demonstrated that surface-based brain mapping could offer more advantages to the study of both local and global properties of the human brain over volume-based one, providing anatomical features such as the cortical thickness and geometrical features such as folding patterns (Fischl et al., 1999). Since the intrinsic topology of cerebral cortex is that of a 2D sheet and the considerable amount of cortex is buried within cortical folds (Van Essen and Drury, 1997; Zilles et al., 1988), a surface-based analysis for the cortex should be adapted to the folding patterns of individual brain.

Conclusion

In this study, we have demonstrated that the use of an age-matched pediatric brain template in a pediatric study leads to a considerably different tissue distribution from that obtained with an adult-based template. Compared with the ABT, the average amount of local deformation over segmented tissue regions during non-linear registration was reduced over 20% when using the ePBT. The interpretation of pediatric imaging data based on the template from adult population should be undertaken with circumspection. Template performance was evaluated in terms of various surface and volumetric characteristics of an independent pediatric dataset. The comparison of an external adult with an external pediatric template confirms previous studies that stressed the need for a pediatric template. In addition, we also extended these findings by removing the inherent confound in a comparison of external adult versus internal pediatric template even though there was no significant difference between the internal and external pediatric template.

Acknowledgments

This work was supported by the Korea Research Foundation Grant funded by the Korean Government (MOEHRD) (KRF-2006-214-D00208) and this project has been funded in whole or in part with Federal funds from the National Institute of Child Health and Human Development, the National Institute on Drug Abuse, the National Institute of Mental Health, and the National Institute of Neurological Disorders and Stroke (Contract #s N01-HD02-3343, N01-MH9-0002, and N01-NS-9-2314, -2315, -2316, -2317, -2319 and -2320). Special thanks to the NIH contracting officers for their support.

We also acknowledge the important contribution and remarkable spirit of John Haselgrove, Ph.D. (deceased).

Appendix A. Brain Development Cooperative Group

The MRI Study of Normal Brain Development is a cooperative study performed by six pediatric study centers in collaboration with a Data Coordinating Center (DCC), a Clinical Coordinating Center (CCC), a Diffusion Tensor Processing Center (DPC), and staff of the National Institute of Child Health and Human Development (NICHD), the National Institute of Mental Health (NIMH), the National Institute on Drug Abuse (NIDA), and the National Institute for Neurological Diseases and Stroke (NINDS), Rockville, Maryland. Key personnel from the six pediatric study centers are as follows: Children's Hospital Medical Center of Cincinnati, Principal Investigator William S. Ball, M.D., Investigators Anna Weber Byars, Ph.D., Mark Schapiro, M.D., Wendy Bommer, R.N., April Carr, B.S., April German, B.A., Scott Dunn, R.T.; Children's Hospital Boston, Principal Investigator Michael J. Rivkin, M.D., Investigators Deborah Waber, Ph.D., Robert Mulkern, Ph.D., Sridhar Vajapeyam, Ph.D., Abigail Chiverton, B.A., Peter Davis, B.S., Julie Koo, B.S., Jacki Marmor, M.A., Christine Mrakotsky, Ph.D., M.A., Richard Robertson, M.D., Gloria McAnulty, Ph.D; University of Texas Health Science Center at Houston, Principal Investigators Michael E. Brandt, Ph.D., Jack M. Fletcher, Ph.D., Larry A. Kramer, M.D., Investigators Grace Yang, M.Ed., Cara McCormack, B.S., Kathleen M. Hebert, M.A., Hilda Volero, M.D.; Washington University in St. Louis, Principal Investigators Kelly Botteron, M.D., Robert C. McKinstry, M.D., Ph.D., Investigators William Warren, Tomoyuki Nishino, M.S., C. Robert Almli, Ph.D., Richard Todd, Ph.D., M.D., John Constantino, M.D.; University of California Los Angeles, Principal Investigator James T. McCracken, M.D., Investigators Jennifer Levitt, M.D., Jeffrey Alger, Ph.D., Joseph O'Neil, Ph.D., Arthur Toga, Ph.D., Robert Asarnow, Ph.D., David Fadale, B.A., Laura Heinichen, B.A., Cedric Ireland B.A.; Children's Hospital of Philadelphia, Principal Investigators Dah-Jyuu Wang, Ph.D. and Edward Moss, Ph.D., Investigators Robert A. Zimmerman, M.D., and Research Staff Brooke Bintliff, B.S., Ruth Bradford, Janice Newman, M.B.A. The Principal Investigator of the data coordinating center at McGill University is Alan C. Evans, Ph.D., Investigators Rozalia Arnaoutelis, B.S., G. Bruce Pike, Ph.D., D. Louis Collins, Ph.D., Gabriel Leonard, Ph.D., Tomas Paus, M.D., Alex Zijdenbos, Ph.D., and Research Staff Samir Das, B.S., Vladimir Fonov, Ph.D., Luke Fu, B.S., Jonathan Harlap, Ilana Leppert, B.E., Denise Milovan, M.A., Dario Vins, B.C.,, and at Georgetown University, Thomas Zeffiro, M.D., Ph.D. and John Van Meter, Ph.D. Ph.D. Investigators at the Neurostatistics Laboratory, Harvard University/McLean Hospital, Nicholas Lange, Sc.D., and Michael P. Froimowitz, M.S., work with data coordinating center staff and all other team members on biostatistical study design and data analyses. The Principal Investigator of the Clinical Coordinating Center at Washington University is Kelly Botteron, M.D., Investigators C. Robert Almli Ph.D., Cheryl Rainey, B.S., Stan Henderson M.S.,

Tomoyuki Nishino, M.S., William Warren, Jennifer L. Edwards M.SW., Diane Dubois R.N., Karla Smith, Tish Singer and Aaron A. Wilber, M.S. The Principal Investigator of the Diffusion Tensor Processing Center at the National Institutes of Health is Carlo Pierpaoli, MD, Ph.D., Investigators Peter J. Basser, Ph.D., Lin-Ching Chang, Sc.D., Chen Guan Koay, Ph.D. and Lindsay Walker, M.S. The Principal Collaborators at the National Institutes of Health are Lisa Freund, Ph.D. (NICHD), Judith Rumsey, Ph.D. (NIMH), Lauren Baskir, Ph.D. (NIMH), Laurence Stanford, PhD. (NIDA), Karen Sirocco, Ph.D. (NIDA) and from NINDS, Katrina Gwinn-Hardy, M.D., and Giovanna Spinella, M.D. The Principal Investigator of the Spectroscopy Processing Center at the University of California Los Angeles is James T. McCracken, M.D., Investigators Jeffry R. Alger, Ph.D., Jennifer Levitt, M.D., Joseph O'Neill, Ph.D.

References

Ashburner, J., Friston, K.J., 2000. Voxel-based morphometry—the methods. NeuroImage 11, 805–821.

Bookstein, F.L., 1997. Landmark methods for forms without landmarks: morphometrics of group differences in outline shape. Med. Image Anal. 1, 225–243.

Burgund, E.D., Kang, H.C., Kelly, J.E., Buckner, R.L., Snyder, A.Z., Petersen, S.E., Schlaggar, B.L., 2002. The feasibility of a common stereotactic space for children and adults in fMRI studies of development. NeuroImage 17, 184–200.

Chung, M.K., Worsley, K.J., Robbins, S., Paus, T., Taylor, J., Giedd, J.N., Rapoport, J.L., Evans, A.C., 2003. Deformation-based surface morphometry applied to gray matter deformation. NeuroImage 18, 198–213.

Collins, D.L., Neelin, P., Peters, T.M., Evans, A.C., 1994. Automatic 3D intersubject registration of MR volumetric data in standardized Talairach space. J. Comput. Assist. Tomogr. 18, 192–205.

Courchesne, E., Chisum, H.J., Townsend, J., Cowles, A., Covington, J., Egaas, B., Harwood, M., Hinds, S., Press, G.A., 2000. Normal brain development and aging: quantitative analysis at in vivo MR imaging in healthy volunteers. Radiology 216, 672–682.

Evans, A.C., Brain Development Cooperative Group, 2006. The NIH MRI study of normal brain development. NeuroImage 30, 184–202.

Fischl, B., Sereno, M.I., Tootell, R.B., Dale, A.M., 1999. High-resolution intersubject averaging and a coordinate system for the cortical surface. Hum. Brain Mapp. 8, 272–284.

Genovese, C.R., Lazar, N.A., Nichols, T., 2002. Thresholding of statistical maps in functional neuroimaging using the false discovery rate. NeuroImage 15, 870–878.

Giedd, J.N., Blumenthal, J., Jeffries, N.O., Castellanos, F.X., Liu, H., Zijdenbos, A., Paus, T., Evans, A.C., Rapoport, J.L., 1999. Brain development during childhood and adolescence: a longitudinal MRI study. Nat. Neurosci. 2, 861–863.

Good, C.D., Johnsrude, I., Ashburner, J., Henson, R.N.A., Friston, K.J., Frackowiak, R.S.J., 2001. Cerebral asymmetry and the effects of sex and handedness on brain structure: a voxel-based morphometric analysis of 465 normal adult human brains. NeuroImage 14, 685–700.

Grabner, G., Janke, A.L., Budge, M.M., Smith, D., Pruessner, J., Collins, D.L., 2006. Symmetric atlasing and model based segmentation: an application to the hippocampus in older adults. Med. Image Comput. Comput.-Assist. Interv. - Miccai 4191 (Pt. 2), 58–66.

Guimond, A., Meunier, J., Thirion, J.P., 2000. Average brain models: a convergence study. Comput. Vis. Image Underst. 77, 192–210.

Hoeksma, M.R., Kenemans, J.L., Kemner, C., van Engeland, H., 2005. Variability in spatial normalization of pediatric and adult brain images. Clin. Neurophysiol. 116, 1188–1194.

Im, K., Lee, J.M., Lyttelton, O., Kim, S.H., Evans, A.C., Kim, S.I., 2008. Brain size and cortical structure in the adult human brain. Cereb. Cortex 18, 2181–2191.

Kabani, N., Le Goualher, G., MacDonald, D., Evans, A.C., 2001. Measurement of cortical thickness using an automated 3-D algorithm: a validation study. NeuroImage 13, 375–380.

Kim, J.S., Singh, V., Lee, J.K., Lerch, J., Ad-Dab'bagh, Y., MacDonald, D., Lee, J.M., Kim, S.I., Evans, A.C., 2005. Automated 3-D extraction and evaluation of the inner and outer cortical surfaces using a Laplacian map and partial volume effect classification. NeuroImage 27, 210–221.

Kiselev, V.G., Hahn, K.R., Auer, D.P., 2003. Is the brain cortex a fractal? NeuroImage 20, 1765–1774.

Lange, N., Giedd, J.N., Castellanos, F.X., Vaituzis, A.C., Rapoport, J.L., 1997. Variability of human brain structure size: ages 4–20 years. Psychiatry Res. 74, 1–12.

Lee, J.K., Lee, J.M., Kim, J.S., Kim, I.Y., Evans, A.C., Kim, S.I., 2006. A novel quantitative cross-validation of different cortical surface reconstruction algorithms using MRI phantom. NeuroImage 31, 572–584.

Lerch, J.P., Evans, A.C., 2005. Cortical thickness analysis examined through power analysis and a population simulation. NeuroImage 24, 163–173.

Lotjonen, J., Reissman, P.J., Magnin, I.E., Nenonen, J., Katila, T., 1998. A triangulation method of an arbitrary point set for biomagnetic problems. IEEE Trans. Magn. 34, 2228–2233.

Lyttelton, O., Boucher, M., Robbins, S., Evans, A., 2007. An unbiased iterative group registration template for cortical surface analysis. NeuroImage 34, 1535–1544.

MacDonald, D., Kabani, N., Avis, D., Evans, A.C., 2000. Automated 3-D extraction of inner and outer surfaces of cerebral cortex from MRI. NeuroImage 12, 340–356.

Machilsen, B., d'Agostino, E., Maes, F., Vandermeulen, D., Hahn, H.K., Lagae, L., Stiers, P., 2007. Linear normalization of MR brain images in pediatric patients with periventricular leukomalacia. NeuroImage 35, 686–697.

Mazziotta, J.C., Toga, A.W., Evans, A., Fox, P., Lancaster, J., 1995. A probabilistic atlas of the human brain: theory and rationale for its development. The International Consortium for Brain Mapping (ICBM). NeuroImage 2, 89–101.

Miller, M., Banerjee, A., Christensen, G., Joshi, S., Khaneja, N., Grenander, U., Matejic, L., 1997. Statistical methods in computational anatomy. Stat. Methods Med. Res. 6, 267–299.

Muzik, O., Chugani, D.C., Juhasz, C., Shen, C., Chugani, H.T., 2000. Statistical parametric mapping: assessment of application in children. NeuroImage 12, 538–549.

Pfefferbaum, A., Mathalon, D.H., Sullivan, E.V., Rawles, J.M., Zipursky, R.B., Lim, K.O., 1994. A quantitative magnetic resonance imaging study of changes in brain morphology from infancy to late adulthood. Arch. Neurol. 51, 874–887.

Shaw, P., Greenstein, D., Lerch, J., Clasen, L., Lenroot, R., Gogtay, N., Evans, A., Rapoport, J., Giedd, J., 2006. Intellectual ability and cortical development in children and adolescents. Nature 440, 676–679.

Sled, J.G., Zijdenbos, A.P., Evans, A.C., 1998. A nonparametric method for automatic correction of intensity nonuniformity in MRI data. IEEE Trans. Med. Imaging 17, 87–97.

Smith, S.M., 2002. Fast robust automated brain extraction. Hum. Brain Mapp. 17, 143–155.

Talairach, J., Tournoux, P., 1988. Co-planar Stereotaxic Atlas of the Human Brain: 3-Dimensional Proportional System—An Approach to Cerebral Imaging. Thieme Medical Publishers, New York.

Thompson, P.M., Giedd, J.N., Woods, R.P., MacDonald, D., Evans, A.C., Toga, A.W., 2000a. Growth patterns in the developing brain detected by using continuum mechanical tensor maps. Nature 404, 190–193.

Thompson, P.M., Mega, M.S., Narr, K.L., Sowell, E.R., Blanton, R.E., Toga, A.W., 2000b. Brain Image Analysis and Atlas Construction. SPIE Press, Bellingham.

Thompson, P.M., Lee, A.D., Dutton, R.A., Geaga, J.A., Hayashi, K.M., Eckert, M.A., Bellugi, U., Galaburda, A.M., Korenberg, J.R., Mills, D.L., Toga, A.W., Reiss, A.L., 2005. Abnormal cortical complexity and thickness profiles mapped in Williams syndrome. J. Neurosci. 25, 4146–4158.

Toga, A.W., Thompson, P.M., 2001. The role of image registration in brain mapping. Image Vis. Comput. 19, 3–24.

Tohka, J., Zijdenbos, A., Evans, A., 2004. Fast and robust parameter estimation for statistical partial volume models in brain MRI. NeuroImage 23, 84–97.

Van Essen, D.C., Drury, H.A., 1997. Structural and functional analyses of human cerebral cortex using a surface-based atlas. J. Neurosci. 17, 7079–7102.

Van Essen, D.C., Dierker, D., Snyder, A.Z., Raichle, M.E., Reiss, A.L., Korenberg, J., 2006. Symmetry of cortical folding abnormalities in Williams syndrome revealed by surface-based analyses. J. Neurosci. 26, 5470–5483.

Wilke, M., Schmithorst, V.J., Holland, S.K., 2002. Assessment of spatial normalization of whole-brain magnetic resonance images in children. Hum. Brain Mapp. 17, 48–60.

Wilke, M., Schmithorst, V.J., Holland, S.K., 2003. Normative pediatric brain data for spatial normalization and segmentation differs from standard adult data. Magn. Reson. Med. 50, 749–757.

Wilke, M., Holland, S.K., Altaye, M., Gaser, C., 2008. Template-O-Matic: a toolbox for creating customized pediatric templates. Neuroimage 41, 903–913.

Yoon, U., Lee, J.M., Im, K., Shin, Y.W., Cho, B.H., Kim, I.Y., Kwon, J.S., Kim, S.I., 2007. Pattern classification using principal components of cortical thickness and its discriminative pattern in schizophrenia. NeuroImage 34, 1405–1415.

Zijdenbos, A.P., Forghani, R., Evans, A.C., 2002. Automatic "pipeline" analysis of 3-D MRI data for clinical trials: application to multiple sclerosis. IEEE Trans. Med. Imaging 21, 1280–1291.

Zilles, K., Armstrong, E., Schleicher, A., Kretschmann, H.J., 1988. The human pattern of gyrification in the cerebral cortex. Anat. Embryol. (Berl) 179, 173–179.